Received: 17 January 2020 | Revised: 14 May 2020 | Accepted: 14 May 2020

DOI: 10.1002/pc.25669

RESEARCH ARTICLE

Polymer COMPOSITES WILEY

Mechanical, thermal, and micro- and nanostructural properties of polyvinyl chloride/graphene nanoplatelets nanocomposites

Ferda Mindivan[1,2] | **Meryem Göktaş**[2,3] | **Ali S. Dike**[4]

[1]Faculty of Engineering, Department of Bioengineering, Bilecik Seyh Edebali University, Bilecik, Turkey

[2]Biotechnology Application and Research Center, Bilecik Seyh Edebali University, Bilecik, Turkey

[3]Vocational College, Department of Metallurgy, Bilecik Seyh Edebali University, Bilecik, Turkey

[4]Faculty of Engineering, Department of Materials Engineering, Adana Alpaslan Türkeş Science and Technology University, Adana, Turkey

Correspondence
Ferda Mindivan, Faculty of Engineering, Department of Bioengineering, Bilecik Seyh Edebali University, Bilecik 11230, Turkey.
Email: ferda.mindivan@bilecik.edu.tr

Abstract

This article describes micro- and nanostructural, mechanical, and thermal properties of nanocomposites based on polyvinyl chloride (PVC) and graphene nanoplatelets (GNP). The primary objective of this study was to extend restricted application area of PVC due to its low thermal stability and limited mechanical properties. GNP-filled PVC nanocomposites were prepared (0, 0.1, 0.3, 0.5, and 1.0 wt%) by colloidal blending method and characterized in detail. The highest value of the tensile strength 13.73 MPa (an increase of 58%) and the highest value of microhardness 83.42 MPa (an increase of 82%) were obtained with GNP loading content of 0.5 wt% compared neat PVC. The mechanical properties started to decrease at loading higher than 0.5 wt%; however, the thermal properties continued to increase. The differential scanning calorimetry and Fourier transform infrared analysis results of this nanocomposite confirmed that the increase in glass transition temperature from 34.99°C to 44.36°C and the decrease in the height of functional groups peaks proved to prevented segmental relaxation and intermolecular vibrations of PVC, respectively. Thermogravimetric analysis results were showed that the percentage of carbonaceous residue increased to 15.77% by increasing the GNP content from 0.1 to 0.5 wt%. As a result, the best GNP loading was at 0.5 wt% for PVC/GNP nanocomposites where mechanical and thermal properties of PVC/GNP were both enhanced.

KEYWORDS

graphene nanoplatelets, mechanical properties, nanocomposite, polyvinyl chloride, thermal stability

1 | INTRODUCTION

The current research studies in the nanocomposite materials focus on the improvement of the physical, mechanical, thermal, and electrical properties of them.[1] One of the most precious products of the chemical industry and the common thermoplastic material worldwide is polyvinyl chloride (PVC). The major reason for preference of PVC is that it is lightweight and naturally resistant to chemical attacks due to its high stiffness and high resistance to most acids and many other chemicals.[2] Moreover, PVC is cheap, which makes it competitive for commercial use.[3] Many commercial products such as pipes, films, and gloves are made of PVC.[4] However, its low thermal stability and poor mechanical properties restrict its application areas.[5] Graphene nanoplatelets (GNP) and their composites with polymer nowadays attracted particular interest.[6] GNP are short stacks of

individual layers of graphene attached by van der Waals forces, which increase the tensile stiffness of composite materials.[6,7] Because of graphene's unparalleled thermal and mechanical properties, studies in the literature report its use in various applications with the epoxy matrix,[8–11] polypropylene,[12] poly(ether ketone),[13] and high-density polyethylene (HDPE)[14] matrixes. But to the best of authors' knowledge, GNP-based nanocomposites have not been investigated yet in PVC matrix without additives (plasticizers, fillers, or stabilizers). Wang et al used commercial multilayer graphene as reinforcing fillers, in order to improve mechanical properties[15] and tribological performance[16] of soft-PVC composites. Deshmukh and Joshi showed the mechanical, thermal, and electrical characterization of graphene oxide (GO)-reinforced PVC nanocomposites.[17] Akhina et al obtained flexible composites with PVC/reduced GO (RGO).[18] In previous studies we have observed that the structural, thermal, and mechanical properties of PVC composites containing GO[19] and RGO[5] at different weight percentages. These studies showed that the amount of oxygen containing functional groups has not improved the thermal and mechanical properties as expected. Therefore, in this study GNP was used as filler to prepare nanocomposites and investigated micro- and nanostructures, thermal, and mechanical properties. Harmless plasticizers or stabilizers were not used to increase potential application areas of PVC at medical market materials. In addition, the colloidal blending method was used in this study because this method is the most common, cost effective, and practical.

2 | EXPERIMENTAL

2.1 | Materials

Tetrahydrofuran (THF) was of reagent grade and purchased from Merck. GNP was obtained from Grafen Chemical Industries, Turkey (thickness ~5 nm-8 nm and lateral dimension ~5 nm).

2.2 | Preparation of nanocomposites

Figure 1 illustrates the preparation of PVC/GNP nanocomposites by a colloidal blending method. PVC was first dissolved in THF at 60 C to 70°C and the resulting PVC solution was poured into a glass petri dish and kept in an oven at 70°C for slow evaporation of the THF to prepare neat PVC. To prepare PVC/GNP nanocomposites, GNP powder was dispersed and PVC was dissolved in THF by separate beakers and dispersed GNP powder was sonicated for 30 minutes at room temperature. These two solutions were mixed and the mixture was further sonicated for 1 hour. The obtained homogeneous dispersion was poured onto a glass petri dish and kept in an oven at 70°C for slow evaporation of the THF. The GNP content in the PVC/GNP nanocomposite was varied from 0.1 to 1.0 wt%. The resulting nanocomposites were labeled PVC/GNP*x*, where *x* is the wt% of GNP.

2.3 | Characterization techniques

Fourier transform infrared (FTIR) spectroscopy of PVC/GNP nanocomposites was carried out with FTIR spectrophotometer (Spectrum 100, Perkin Elmer) in the wave number range 400 to 4000 cm^{-1} in a transmittance mode. X-ray diffraction (XRD) data were obtained using a PAN analytical Empyrean diffractometer equipped with Cu-Ka source (λ = 1.5404 Å). The scans were obtained in a 2θ range from 5 to 60, with a 0.1 step size. The crystallite size of the nanocomposites was calculated by the following Scherrer Equation (1)[20] and the lattice strain, ε, was calculated based on Equation (2)[21]:

$$L = \frac{K\ddot{A}n\lambda}{\beta\ddot{A}n\mathrm{Cos}\,\theta}, \quad (1)$$

$$\varepsilon = \frac{\beta}{4.\tan\theta}, \quad (2)$$

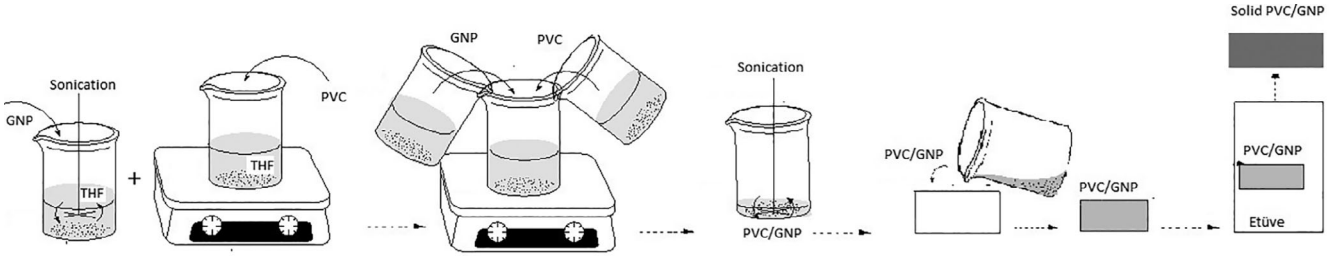

FIGURE 1 A schematic illustration of the fabrication of nanocomposites. GNP, graphene nanoplatelets; PVC, polyvinyl chloride; THF, tetrahydrofuran

where L is the crystallite size, K is a constant related to crystallite shape, β is the full width at half maximum, λ is the wave length, and θ is the peak position. In order to examine the thermal stability of the composites, thermogravimetric analysis (TGA) was performed on a Hitachi STA 7300, operated in nitrogen atmosphere at a heating rate of 10°C/min. In order to measure the glass transition temperature (T_g) of the samples prepared, differential scanning calorimetry (DSC) analysis was performed using a Hitachi DSC 7000X, operated in nitrogen atmosphere at a heating rate of 10°C/min. Field emission scanning electron microscopy (FE-SEM) images of the samples were obtained with a Supra 40VP, Zeiss. The investigation of interface nanostructure of the nanocomposites was done by high-resolution transmission electron microscopy (HRTEM, JEOL 2100). The tensile tests were performed based on the ASTM D 3822 standard procedure[22] by a tensile testing machine (Lloyd LR 5 K) with a load cell of 10 N and the strain rate of 20 mm/min. At least five measurements with standard deviations were applied for each sample. Microhardness of nanocomposites was measured on the metallographic samples using a Knoop indenter under a load of 10 g.

3 | RESULTS AND DISCUSSION

3.1 | Structural properties

3.1.1 | FTIR spectroscopy

FTIR spectra of the neat PVC and prepared PVC/GNP nanocomposites over wavenumbers from 4000 to 400 cm^{-1} are shown in Figure 2. FTIR spectra of all samples were recorded in the transmittance mode and the band assignments for samples are listed in Table 1. The bands at 2950 to 2908 cm^{-1} and 1426 to 1333 cm^{-1} represented the CH stretching and the CH_2 deformation band in the neat PVC, respectively.[7,23,24] The band of the CH rocking in the neat PVC were observed in the 1254 cm^{-1}.[24,25] For neat PVC, *trans* CH wagging band could be observed at 957 cm^{-1}.[6,23,24] In addition, the characteristic peaks of neat PVC were observed CCl stretching vibration at 834 cm^{-1}[7,24,26] and *cis* CH wagging at 608 cm^{-1},[6,24,25] respectively. The comparison of the FTIR spectra of neat PVC and different loading content of PVC/GNP nanocomposites (0.1, 0.3, 0.5, and 1.0 wt%) is presented in Figure 2 and Table 1. The characteristic peaks of PVC/GNP nanocomposites responsible for CH stretching, CH_2 deformation, CH rocking, *trans* CH wagging, CCl stretching as well as *cis* CH wagging were clearly observed over the spectra for all nanocomposites and no new peak was formed.[2,6] The band at 1739 cm^{-1} corresponds to the CO stretching of neat PVC (Figure 2); the same band also appeared with much low intensity in the spectra of all nanocomposites, indicating the entrance of the GNP to the PVC matrix.[7] As seen from Table 1, significant change was not observed in the wavenumbers of the PVC/GNP nanocomposites compared with neat PVC. However, the FTIR spectra of the all nanocomposites showed a decrease in the height of functional groups peaks. It also could be found that the intensities of peaks in PVC/GNP0.5 nanocomposite was lower in comparison to neat PVC and other nanocomposites. This result indicated that loading content 0.5 wt% of GNP prevented intermolecular vibrations of PVC.[3] Our previous work revealed that there was no marked difference in the FTIR spectra for all composites as the loading content GO increases.[19] The performance of GNP was better than GO because of better dispersion and exfoliation degree of nanoplatelets and better interfacial interaction between nanoplatelets and PVC are important factors in enhancing the structural properties of nanocomposite samples.

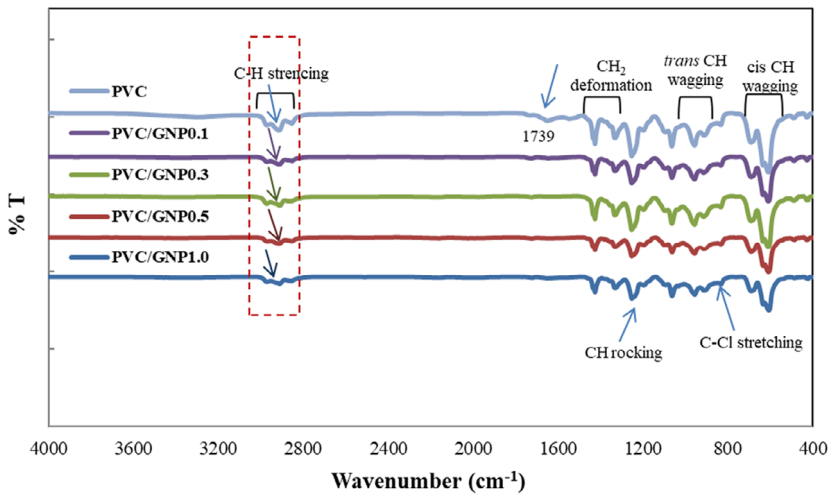

FIGURE 2 The FTIR spectra of neat PVC and the PVC/GNP nanocomposites. FTIR, Fourier transform infrared; GNP, graphene nanoplatelets; PVC, polyvinyl chloride [Color figure can be viewed at wileyonlinelibrary.com]

TABLE 1 Vibrational modes and wavenumbers of neat PVC and the PVC/GNP nanocomposites

Samples Vibrational modes	Neat PVC Wavenumbers (cm^{-1})	PVC/GNP0.1	PVC/GNP0.3	PVC/GNP0.5	PVC/GNP1.0
C—H stretching	2916	2912	2912	2913	2910
CH_2 deformation	1333	1332	1332	1330	1333
CH rocking	1254	1253	1254	1253	1252
trans CH wagging	957	955	956	955	956
C—Cl stretching	834	833	833	832	832
cis CH wagging	608	604	607	607	605
—C═O stretching	1739	1728	1724	1720	1723

Abbreviations: GNP, graphene nanoplatelets; PVC, polyvinyl chloride.

3.1.2 | XRD analysis

The XRD patterns were evaluated to define the morphology and distribution of introduced GNP in the PVC/GNP nanocomposites. The XRD patterns of neat PVC and PVC/GNP nanocomposites are plotted in Figure 3. No diffraction pattern was observed in the neat PVC, as shown in Figure 3, which proved the presence of amorphous phase.[27] The addition of GNP yielded to the existence of a new peak, confirming the presence of GNP in nanocomposites. XRD patterns of all PVC/GNP nanocomposites showed diffraction peaks at $2\theta = 26.7°$ (from GNP)[1] which is associated with graphitic (002) plane[28] and $2\theta = 29.2°$ (Figure 3). In all of the PVC/GNP nanocomposite cases, sharp peaks for GNP were observed, and the diffraction intensity of the GNP peaks became stronger as the amount of GNP increased in proportion to PVC, which is consistent with that of polymer composites with GNP reported in the literature.[23] Ma et al[29] suggested that the diffraction (002) at 26.6 showed the graphene layers in each platelet because the diffraction intensity increased at higher GNP contents at epoxy nanocomposites Pirayesh et al[30] identified that intensity of the XRD peak of nanocomposites decreased by increasing the amount of epoxy-containing GO nanosheets and did not show the characteristic peak of the nanosheets. They explained that structural order of the polymer and the proper dispersion of nanosheets were destroyed by adding further nanosheets into the polymeric matrix. This phenomenon indicated good interaction between GNP particles and PVC matrix[28] and it is evident that the introduced filler particles uncovered crystalline regions in the polymer matrix of nanocomposites. The values of d-spacing, crystallite size, and microstrain of nanocomposites with different content of GNP, (0.1%, 0.3%, 0.5%, and 1.0%) for $2\theta = 26.7°$, are shown in Table 2. Inclusion of fillers affected the structural state of nanocomposites and formed crystalline

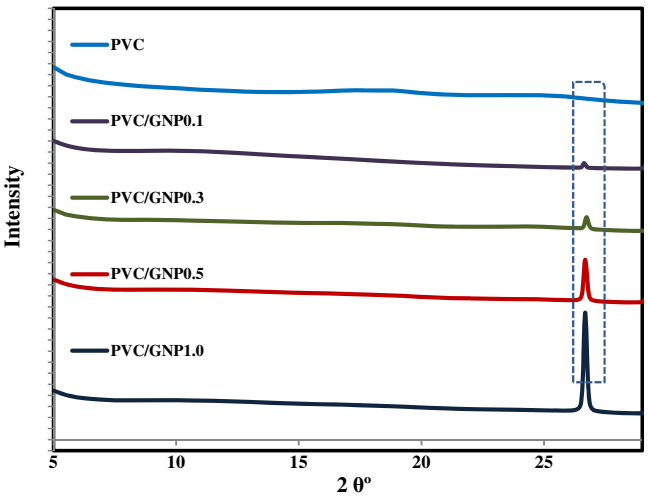

FIGURE 3 X-ray diffraction patterns of neat PVC and PVC/GNP nanocomposites. GNP, graphene nanoplatelets; PVC, polyvinyl chloride [Color figure can be viewed at wileyonlinelibrary.com]

structure compared to amorphous PVC. It is observed that 0.3%, 0.5%, and 1.0% GNP contents result in reduction of crystallite size achieving 38.6%, for comparison with 0.1% GNP. The results of crystallite size revealed that the incorporation of GNP improved the crystallinity in the PVC/GNP0.1 nanocomposite because GNP could act as nucleation centers, which help increasing crystallinity of polymer matrix. Rafeie et al[31] reported the GNP acted as nucleating agent in poly(vinylidene fluoride) component.

The reduction of the crystallite size is associated with the presence of 0.3%, 0.5%, and 1.0% GNPs nanoparticles, which bind polymer chains.[32] It is further observed that the microstrain is little increased by increasing the GNPs content. Amangah et al[33] investigated the crystallinity of synthesized nanocomposites with modified GO nanoplatelets (mGO) and used by XRD and DSC. They reported that nanoplatelets acted as nucleating agents, which help increasing

TABLE 2 d-Spacing, crystallite size, and micro-strain of PVC/GNP nanocomposites. The values are the average values calculated from $2\theta = 26.7^\circ$ peak

GNP content	D-spacing (Å)	Crystallite size (nm)	Microstrain (%)
0.1	3.3459	115.16	0.14527
0.3	3.3374	83.06	0.20089
0.5	3.3407	83.06	0.20110
1	3.3441	83.06	0.20131

Abbreviations: GNP, graphene nanoplatelets; PVC, polyvinyl chloride.

crystallinity of polymer in lower amounts of mGO but in higher amount of mGO, nanoplatelets disrupted reorganization and chain folding during crystallization process. Similarly, in this study, the presence of 0.3%, 0.5%, and 1.0% GNP affected reorganization and chain folding because these amounts of GNP caused binding of polymer chains and too little change of microstrain values. Further, these results also explained the similarity of the d-spacing values in Table 2.

3.2 | Morphological characterization

The morphology of neat PVC and PVC/GNP nanocomposites is shown in Figure 4. The surface morphology of PVC/GNP0.1 composite are similar to that of PVC/GNP0.3 composite and they have bubble-like structure which widely known as ripple but the surface of PVC/GNP0.3 had irregular pits compared with other nanocomposites. The surface image of PVC/GNP0.5 exhibited flattening tendency but PVC/GNP1.0 had smooth surface as neat PVC. According to XRD analysis results, when the loading content is 0.1 wt%, GNP created nucleation centers. Heterogeneous nucleation rate (J) and the energy barrier (ΔG) based on classical nucleation theories are expressed as, respectively[34]:

$$J = J_0 \exp\left(-\frac{\Delta G^*}{kT}\right), \tag{3}$$

$$\Delta G^* = \frac{16\pi\gamma^3 f(\theta)}{3\Delta G^2}. \tag{4}$$

Considering Equations (3) and (4), in the lowest filler content (0.1 wt%), energy barrier was not achieved and nucleation rate increased by decreasing the surface area. However, in 0.3 wt% and other filler contents (0.5 and 1.0 wt%) of GNP, the barrier increased and nucleation decreased because high GNP contents showed an effect increasing surface area.[34] The nucleation of GNP in PVC/GNP0.1 nanocomposite and the dispersion of GNP was identified by TEM, as shown in Figure 4. It was observed that homogeneous dispersion of GNP in the PVC matrix was achieved at all nanocomposites, which can effectively improve the matrix properties. TEM images revealed that when the loading content was 0.1 wt% GNP, regular alignment of dark color layers (see dashed circles in Figure 4) and interlayer distance of layers (see yellow straight line in Figure 4) were seen clearly. As seen from TEM images of PVC/GNP nanocomposites, dark color traces of GNP decreased and lines indicating interlayer distance of layers disappeared with increase of GNP loading content.

3.3 | Thermal characterization

In order to examine the thermal stability of neat PVC and PVC/GNP nanocomposites, DSC, and TGA measurements were carried out. The effect of GNP on the glass transition behavior of PVC matrix was studied using DSC. The DSC curves and T_g of the neat PVC and the nanocomposites containing different weight loadings of GNP are given in Figure 5. Neat PVC and PVC/GNP nanocomposites exhibited one endothermic peak with a melting point. As shown in Figure 5, in comparison to the neat PVC with a melting temperature of 282°C, the PVC/GNP0.5 and the PVC/GNP1.0 nanocomposites showed higher melting temperature values. Thus, it is reasonable to attribute the significant improvement of thermal stability for PVC/GNP0.5 and the PVC/GNP1.0 nanocomposites to the strong interactions between filler/polymer interface and homogeneous dispersion of filler in the polymer matrix. Furthermore, in Figure 5, by increasing the GNP content T_g of nanocomposites, showed a rising trend and the increase in T_g was indicative of a restriction in segmental relaxation. However, neat PVC showed higher T_g value than all nanocomposites which related to the formation of hydrogen bonds between GNP and PVC in nanocomposites. The hydrogen bonds in neat PVC are weaker than the bonds in all nanocomposites because GNP strongly affected to the hydrogen bond.[35] When the loading content is 0.5 and 1.0 wt% GNP, GNP particles dispersed to the amorphous regions of the PVC molecule and caused low degree of crystallinity, which is also consistent with the known literature data.[32] To better elaborate this phenomenon, a schematic diagram of the

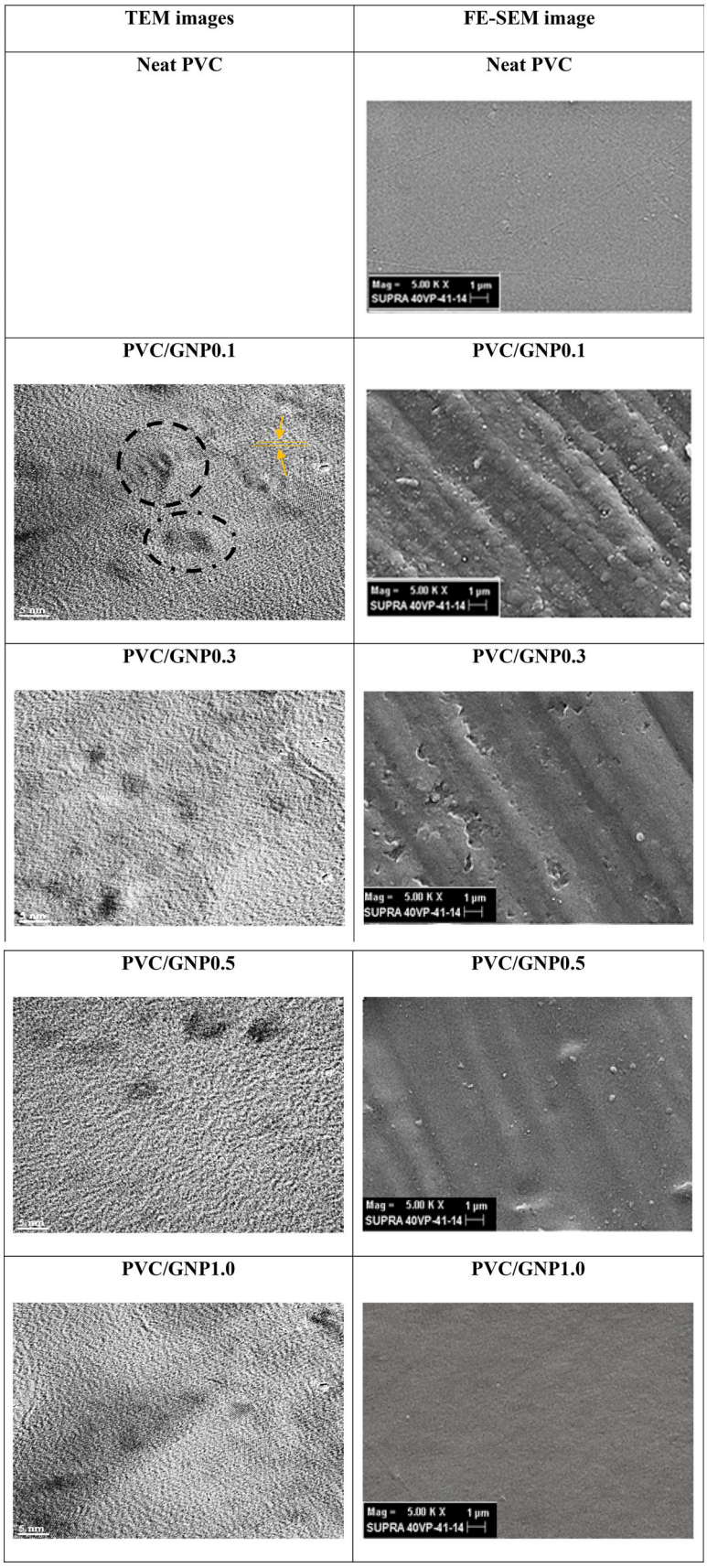

FIGURE 4 FE-SEM images of neat PVC and PVC/GNP nanocomposites (magnification 5 000 k×) and HRTEM images of PVC/GNP nanocomposites (5 nm). FE-SEM, field emission scanning electron microscope; GNP, graphene nanoplatelets; HRTEM, high-resolution transmission electron microscopy; PVC, polyvinyl chloride [Color figure can be viewed at wileyonlinelibrary.com]

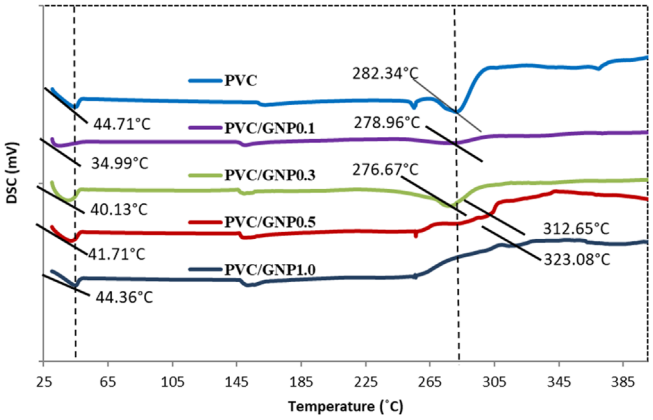

FIGURE 5 DSC curves of the neat PVC and PVC/GNP nanocomposites. DSC, differential scanning calorimetry; GNP, graphene nanoplatelets; PVC, polyvinyl chloride [Color figure can be viewed at wileyonlinelibrary.com]

structural change of PVC nanocomposites by incorporation of GNP is proposed in Figure 6.

The TG and differential thermogravimetry (DTG) curves of neat PVC and PVC/GNP nanocomposites containing different weight loadings of GNP under nitrogen atmosphere are displayed in Figures 7 and 8, respectively, and the experimentally generated results are listed in Table 3. As shown in Figure 7, a three-stage decomposition process could be observed for all the samples. In the first stage of 141 C to 155°C with the corresponding DTG peak temperatures (T_1) (Figure 8), a small amount of weight change was occurred in TGA curve (3%-4%) because of release of water from the chains of polymer.[36] The PVC/GNP nanocomposites showed lower first decomposition temperatures (T_1) than neat PVC because the introduction of GNP to the PVC matrix facilitated the removal of water from the structure (Figure 7). In addition, the main (second) decomposition temperatures (T_2) were shifted to higher values at the all nanocomposites, especially at the nanocomposites with 0.5 and 1.0 wt% loading content of GNP (Figure 8). The weight loss of this second stage could be related to the loss of HCl.[34] It showed higher stability because the GNP did not act as a filler attracting Cl. Therefore, the CCl bonds in PVC were strengthened at this temperature. The main (second) decomposition temperature is very important to understand the interaction mechanism of between PVC and GNP. Bourque et al prepared GNP/HDPE composites and investigated thermal properties. They reported that thermal stability of composites increased with increasing GNP loading but they could not decide whether it was the presence of GNP in the polymer matrix or the modification in the crystalline morphology.[14] In our work, the crystallite size (Table 1) had the highest value for the nanocomposite with 0.1 wt

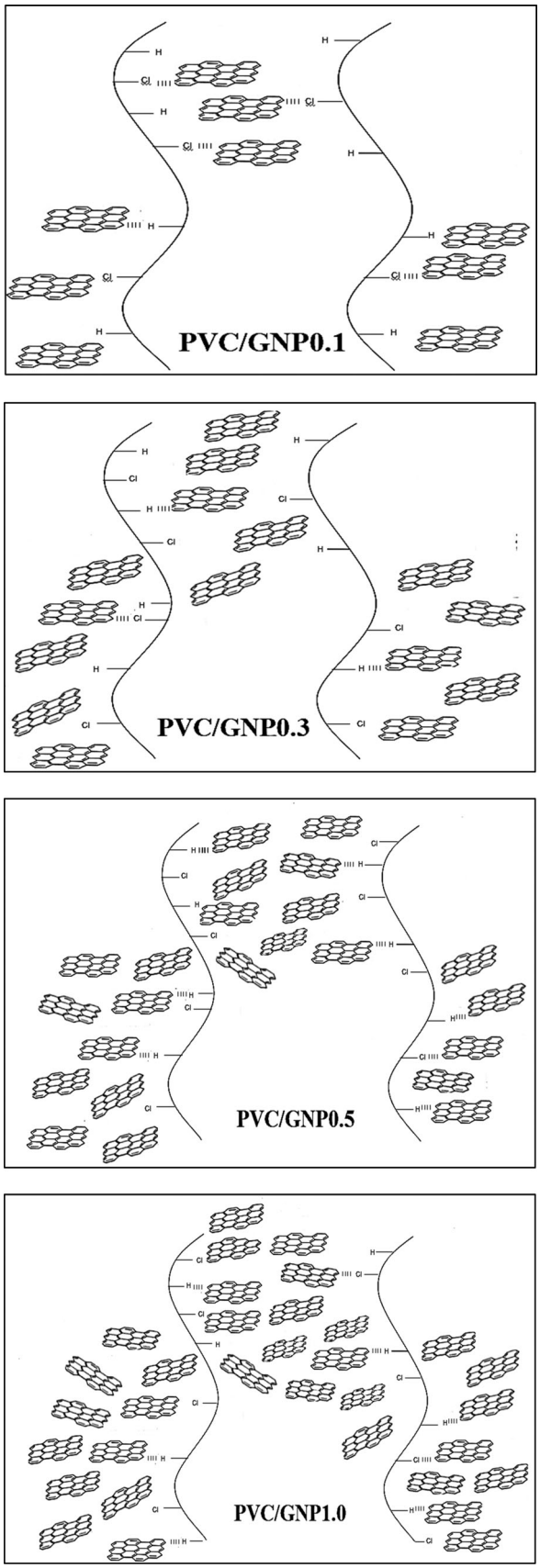

FIGURE 6 The schematic diagram of the structural change of PVC nanocomposites. GNP, graphene nanoplatelets; PVC, polyvinyl chloride

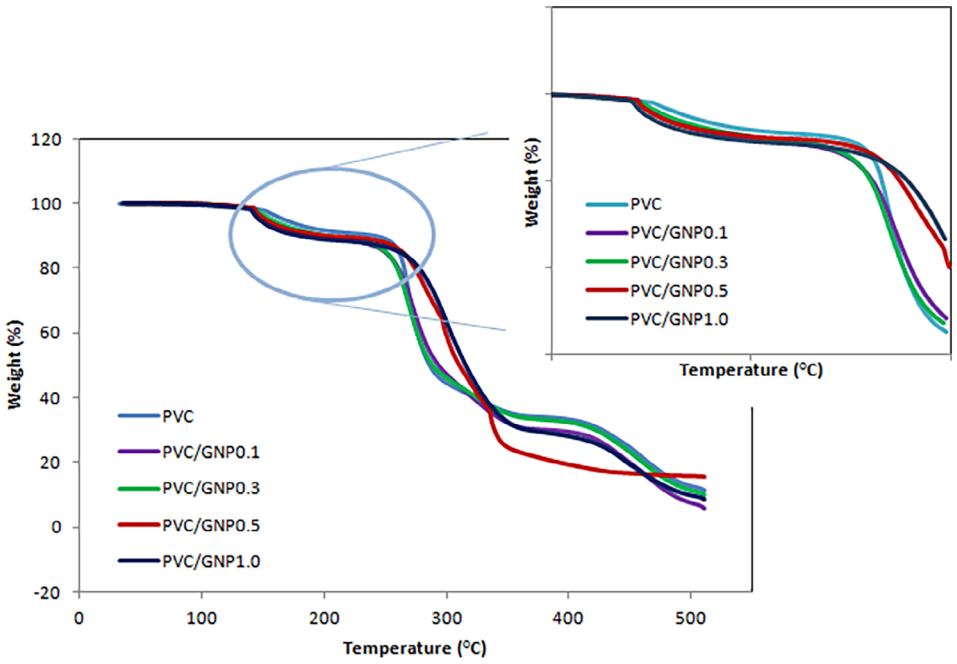

FIGURE 7 A, TG curves of the neat PVC and GNP nanocomposites. B, Zoomed-in plot of TG traces between 200 C and 300°C of the neat PVC and GNP nanocomposites. GNP, graphene nanoplatelets; PVC, polyvinyl chloride; TG, thermogravimetric [Color figure can be viewed at wileyonlinelibrary.com]

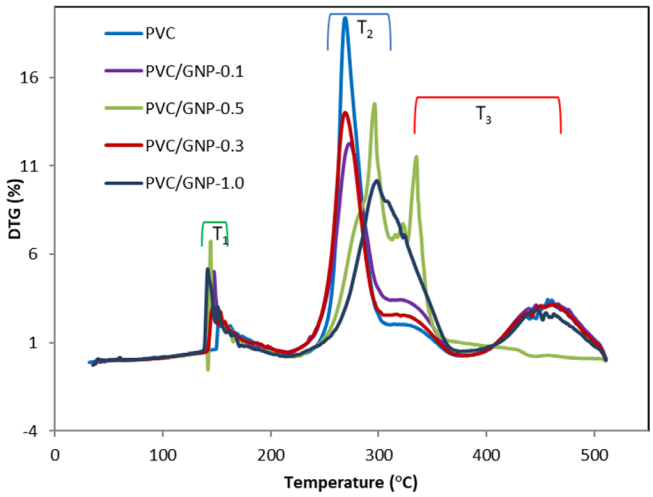

FIGURE 8 DTG curves of neat PVC and PVC/GNP nanocomposites. GNP, graphene nanoplatelets; PVC, polyvinyl chloride [Color figure can be viewed at wileyonlinelibrary.com]

% of GNP, comparing with the other nanocomposites. But the same nanocomposite showed low thermal stability. When the GNP content reached to 0.5 wt% in the PVC matrix, it was seen that thermal stability increased. Therefore, we thought that incorporation of GNP to PVC matrix caused to increase in thermal stability of nanocomposites for this study. The last stage of decomposition is T_3 temperature and resulted in large weight loss (Table 3). It was observed that the percentage of carbonaceous residue increased to 15.77% by increasing the GNP content from 0.1 to 0.5 wt%. According to all thermal analysis results the PVC/GNP0.5 composite had the highest thermal stability was mainly attributed to the great interactions and good compatibility between the GNP and PVC.[37,38]

3.4 | Mechanical characterization

Figures 9 and 10 show the tensile strength and elongation at break (%) results of the nanocomposites, respectively. It is obvious that all samples with GNP showed significant improvement in mechanical properties compared to neat PVC. Tensile strength had a maximum value when the GNP content was 0.5 wt% compared to the neat PVC. Tensile strength for nanocomposite with 0.5 wt% GNP was 13.73 MPa, which is an increment of 58%. This mechanical improvement was mainly attributed to uniform dispersion of GNP in the PVC matrix, and strong GNP-PVC interactions.[39] As seen in Figure 10, for nanocomposites the elongation at break values decreased consistently up to a loading of 0.5 wt%. At 1.0 wt% GNP the tensile strength and elongation at break were almost the same with 0.5 wt% GNP content. The decrease of elongation at break, indicated that the incorporation of GNP led to an increase in brittleness. Mindivan reported similar results between GNP and poliamide 6.[40] High modulus and the specific surface area of GNP affected the tensile properties of the composites.[12,37,41,42] As shown in Figure 11, the PVC/GNP nanocomposites showed much higher microhardness values than the neat PVC. The microhardness of the PVC/GNP0.5 nanocomposite was 83.42 $HK_{0.01}$ (MPa), increasing by 86% in comparison with 45.84 $HK_{0.01}$ (MPa), for the neat

TABLE 3 Thermal parameters for the neat PVC and PVC/GNP nanocomposites (10°C/min heating rate, under N_2 atmosphere)

Sample	T (°C) range			Weight loss at 600°C (%)	Residue at 600°C wt (%)
	T_1	T_2	T_3		
Neat PVC	155.76	270.36	457.28	88.57	11.43
PVC/GNP0.1	147.47	273.91	465.81	94.00	6.00
PVC/GNP0.3	146.97	270.95	457.40	90.19	9.81
PVC/GNP0.5	144.30	296.28	334.25	84.23	15.77
PVC/GNP1.0	141.59	299.83	446.94	91.26	8.74

Abbreviations: GNP, graphene nanoplatelets; PVC, polyvinyl chloride.

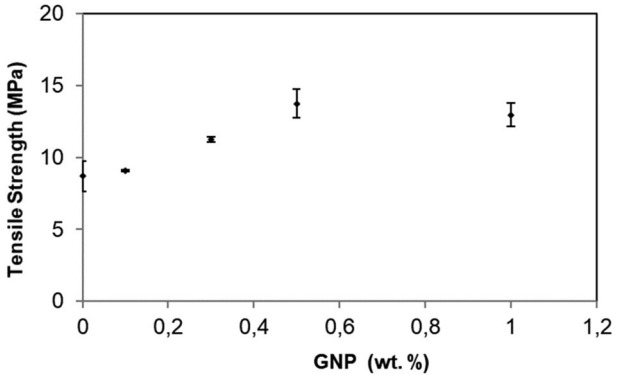

FIGURE 9 The tensile strength of the PVC/GNP nanocomposites. GNP, graphene nanoplatelets; PVC, polyvinyl chloride

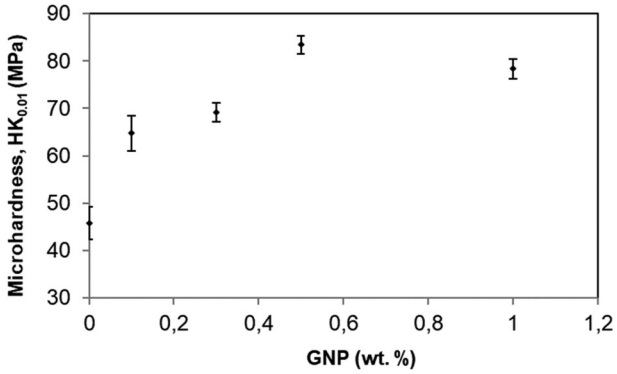

FIGURE 11 The microhardness of the PVC/GNP nanocomposites. GNP, graphene nanoplatelets; PVC, polyvinyl chloride

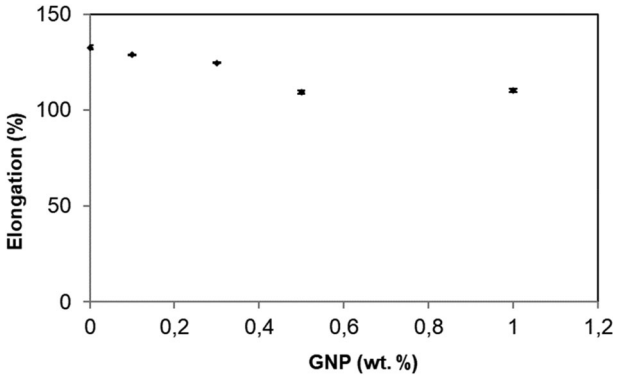

FIGURE 10 The elongation at break of the PVC/GNP nanocomposites. GNP, graphene nanoplatelets; PVC, polyvinyl chloride

PVC. By this way, interfacial interaction increased and thus a more effective load transfer occurred between PVC matrix and filler. According to Puertolas et al, the increase in hardness is associated with the rearrangement of amorphous polymer chains in the surroundings of GNP.[13] In the thermal analysis section, the dispersion of the GNP in amorphous regions of the polymer matrix is discussed by using DSC data. And this increase is due to the morphology change previously observed through SEM images. As the GNP amount further increased, the roughness of surface decreased and the mechanical properties improved as pointed out in Section 3.2.

4 | CONCLUSIONS

In this work, neat PVC and PVC/GNP nanocomposites were prepared by colloidal blending method. The best GNP loading was at 0.5 wt% for PVC/GNP nanocomposites, where both thermal and mechanical properties of nanocomposites were enhanced. This was related to good nanofiller-matrix interaction and homogeneous dispersion. Based on XRD and TEM analysis, the introduce of GNP in the polymer matrix caused to bind polymer chains and lines indicating interlayer distance of layers disappeared with increase of GNP loading content, respectively. Additionally, when the loading content was 0.5 and 1.0 wt% GNP, GNP particles dispersed to the amorphous regions of the PVC molecule, which increases the load transfer between the nanofiller and the polymer matrix. Due to these factors, the tensile strength and microhardness of PVC/GNP0.5

nanocomposite was increased by 45% and 86% at the GNP content of 0.5 wt%, respectively.

CONFLICT OF INTEREST

The authors declare no potential conflict of interest.

ORCID

Ferda Mindivan https://orcid.org/0000-0002-6046-2456
Meryem Göktaş https://orcid.org/0000-0003-1583-8300
Ali S. Dike https://orcid.org/0000-0001-6214-6070

REFERENCES

[1] M. C. Senel, M. Gurbuz, E. Koc, *Compos. Part B* **2018**, *154*, 1.
[2] B. Dan-Asabe, *JKSUES* **2018**, *30*, 296.
[3] H. Wu, T. Li, B. Liu, C. Chen, S. Wang, J. C. Crittenden, *Appl. Surf. Sci.* **2018**, *455*, 987.
[4] M. Khaleghia, K. Didehbana, M. Shabanian, *Ultrason. Sonochem.* **2018**, *43*, 275.
[5] F. Mindivan, M. Göktaş, *Polym. Bull.* **2020**, *77*, 1929.
[6] Y.-S. Jun, J. G. Um, G. Jiang, G. Lui, A. Yu, *Compos. Part B* **2018**, *133*, 225.
[7] O. Aluko, S. Gowtham, G. M. Odegard, *Compos. Struct.* **2018**, *206*, 526.
[8] A. A. Moosa, F. Kubba, M. Raad, A. Ramazani, *Am. J. Mater. Sci.* **2016**, *6*(5), 125.
[9] S. Chatterjee, F. Nafezarefi, N. H. Tai, L. Schlagenhauf, F. A. Nuesch, B. T. T. Chu, *Carbon* **2012**, *50*, 5380.
[10] U. Tayfun, Y. Kanbur, U. Abaci, H. Y. Guney, E. Bayramli, *Compos. Part B: Eng.* **2015**, *80*, 101.
[11] Z. Yu, L. T. Drzal, *Polym. Compos.* **2020**, *41*, 920.
[12] J.-Z. Liang, *Compos. Part B* **2019**, *167*, 241.
[13] J. A. Puertolas, M. Castro, J. A. Morris, R. Ríos, A. Anson-Casaos, *Carbon* **2019**, *141*, 107.
[14] A. J. Bourque, C. R. Locker, A. H. Tsou, M. Vadlamudi, *Polymers* **2016**, *99*, 263.
[15] H. Wang, G. Xie, Z. Ying, Y. Tong, Y. Zeng, J. Mater, *Sci. Technol.* **2015**, *31*, 340.
[16] H. Wang, G. Xie, Z. Zhu, Z. Ying, Y. Zeng, *Compos. Part A* **2014**, *67*, 268.
[17] K. Deshmukh, G. M. Joshi, *Polym. Test.* **2014**, *34*, 211.
[18] H. Akhina, P. M. Arif, M. R. G. Nair, K. Nandakumar, S. Thomas, *Polym. Test.* **2019**, *73*, 250.
[19] F. Mindivan, *Mater. Sci. Non-Equilib. Phase Transform.* **2015**, *3*, 33.
[20] A. Monshi, M. R. Foroughi, M. R. Monshi, *WJNSE* **2012**, *2*, 154.
[21] S. N. Danilchenko, O. G. Kukharenko, C. Moseke, I. Y. Protsenko, L. F. Sukhodub, B. Sulkio-Cleff, *Cryst. Res. Tech.* **2002**, *37*, 1234.
[22] *ASTM D 3822, Standard Test Method for Tensile Properties of Single Textile Fibers*, American Society for Testing and Material, West Conshohocken, PA, **1997**.
[23] A. Wagih, A. Abu-Oqail, A. Fathy, *Ceram. Int.* **2019**, *45*, 1115.
[24] Y. Kanbur, U. Tayfun, *J. Elastom. Plast.* **2019**, *51*, 262.
[25] J. Li, M. Han, Y. Muhammad, Y. Liu, S. Yang, S. Duan, W. Huang, Z. Zhao, *Constr. Build. Mater.* **2018**, *193*, 501.
[26] M. Arab, S. P. H. Marashi, *Tribol. Int.* **2019**, *132*, 1.
[27] M. Yadav, S. Ahmad, F.-C. Chiu, *J. Ind. Eng. Chem.* **2018**, *68*, 246.
[28] M. E. Turan, Y. Sun, Y. Akgul, Y. Turen, H. Ahlatci, *J. Alloys Compd.* **2017**, *724*, 14.
[29] J. Ma, Q. Meng, I. Zaman, S. Zhu, A. Michelmore, N. Kawashima, C. H. Wang, H.-C. Kuan, *Compos. Sci. Technol.* **2014**, *91*, 82.
[30] A. Pirayesh, M. Salami-Kalajahi, H. Roghani-Mamaqani, E. Dehghani, *Prog. Org. Coat.* **2019**, *131*, 211.
[31] O. Rafeie, M. K. R. Aghjeh, A. Tavakoli, M. Salami-Kalajahi, A. Jameie-Oskooie, M. Ghayoumi, *Polym. Compos.* **2019**, *40*, 4402.
[32] I. E. Uflyand, E. G. Drogan, V. E. Burlakovab, K. A. Kydralievac, I. N. Shershnevad, G. I. Dzhardimalievac, *Polym. Test.* **2019**, *74*, 178.
[33] M. Amangah, M. Salami-Kalajahi, H. Roghani-Mamaqani, *Diam. Relat. Mater.* **2018**, *83*, 177.
[34] M. Hasan, M. Leen, *Pro. Nat. Sci. Mater.* **2014**, *24*, 579.
[35] S. W. Kuo, C. F. Huang, F. C. Chang, *J. Polym. Sci. Pol. Phys.* **2001**, *39*, 1348.
[36] N. I. Khan, S. Halder, J. Wang, *Polym. Test.* **2019**, *74*, 138.
[37] H. Wang, G. Xie, M. Fang, Z. Ying, Y. Tong, Y. Zeng, *Compos. Part B* **2015**, *79*, 444.
[38] Y. Wu, Q. Liu, Z. Heng, H. Zou, Y. Chen, M. Liang, *Polym. Compos.* **2019**, *40*, 3866.
[39] H. Wang, G. Xie, M. Fang, Z. Ying, Y. Tong, Y. Zeng, *Compos. Part B* **2017**, *113*, 278.
[40] F. Mindivan, *Tribol. Ind.* **2017**, *39*(3), 277.
[41] T. Guler, U. Tayfun, M. Dogan, E. Bayramli, *Thermochim. Acta* **2017**, *647*, 70.
[42] B. Wang, Q. Fu, Y. Liu, T. Yin, Y. Fu, *Tribol. Int.* **2018**, *123*, 200.

How to cite this article: Mindivan F, Göktaş M, Dike AS. Mechanical, thermal, and micro- and nanostructural properties of polyvinyl chloride/graphene nanoplatelets nanocomposites. *Polymer Composites*. 2020;41:3707–3716. https://doi.org/10.1002/pc.25669